



In-situ preparation of novel nanocomposites of PMMA and ordered mesoporous carbon (FDU-15)

Gholamhossein Mohammadnezhad¹ · Milad Okhovat¹ · Tanin Fazeldehkordi¹ · Mohammad Dinari¹

Received: 6 March 2022 / Accepted: 1 July 2022 / Published online: 9 July 2022
© The Polymer Society, Taipei 2022

Abstract

Ordered mesoporous carbons have recently been in significant attention because of their unique hexagonal structure, tunable large pore volumes, high thermal stability, and high surface-to-volume ratio. In this research paper, for achieving the maximum compatibility between the FDU-15 and poly(methyl methacrylate) (PMMA), 3-aminopropyltriethoxysilane (KH-550) was used as a modifying and coupling agent to facilitate the bond formations between the mesoporous carbon and PMMA with the help of ultrasonic irradiation. Nanocomposite (NC) films were produced via the in-situ polymerization method aligned with various amounts of modified FDU-15. Sample characterizations were done by field-emission scanning electron microscopy (FE-SEM), low angle X-ray diffraction (LXRD), Fourier transform infrared spectroscopy, transmission electron microscopy (TEM), and thermogravimetric analysis (TGA). The LXRD pattern proved that the hexagonal mesoporous structure of FDU-15 was preserved in NCs, however, the intensities of reflexes and long range order were decreased. The PMMA-m-FDU 2 wt% showed the existence of some pores on its surface according to FE-SEM. The TEM images of the NC depicted well-ordered arrays of mesoporous carbon in the PMMA matrix perpendicular to the pore axis and confirmed the 2D structure of the mesopores. TGA data also confirmed that as the m-FDU-15 increases into the PMMA matrix, the higher thermal stability will achieve. Also, the T_d will increase to the higher temperatures. The PMMA-m-FDU 2 wt% showed the highest thermal resistant among the other studied NCs.

Keywords PMMA · Ordered mesoporous carbon (FDU-15) · KH-550 · In-situ polymerization · Thermogravimetric analysis · Modification

Introduction

Poly(methyl methacrylate) (PMMA) is a synthetic thermoplastic polymer which is obtained through addition polymerization of methyl methacrylate (MMA). PMMA shows a unique combination of properties such as transparency, lightweight, and low coefficient of thermal expansion, which makes it a suitable alternative for typical glasses [1, 2]. PMMA can also serve as an inexpensive alternative for polycarbonates (PCs) as it offers some additional benefits, like the polishability, capability for laser cutting, and the absence of toxic bisphenol-A in its chain structure, which is crucial factor for biomedical applications [3, 4]. For instance, in the study conducted by Li et al. the addition of

PMMA to the porous structure of Ti-Mo-Cu alloys resulted in a significant enhancement in the compressive strength of the material used for the tissue engineering purposes [5]. On the other hand, PMMA features some drawbacks in its pure state, notably brittleness, scratch sensitivity, and inferior resistance to strong solvents that limits its potential applications. Therefore, it must be combined with some fillers to compensate its drawbacks [6–8]. In this regard, mesoporous organic materials (MOMs) are among fillers that are widely used due to their extremely high surface to volume ratio, high mechanical and thermal stability, and inertness in chemical environment. The structure of MOMs consist of well-ordered arrays of uniform channels with 2–50 nm. MOMs are accessible in the form of powder, foam, and fiber, which makes them applicable in a variety of applications, namely adsorption of dyes and heavy metals for water treatment [9, 10]. Likewise, ordered mesoporous carbons (OMCs) are porous materials with interconnected channels with high surface to volume ratio, significant chemical and thermal stability, and

✉ Gholamhossein Mohammadnezhad
mohammadnezhad@iut.ac.ir; g_m1358@yahoo.com

¹ Department of Chemistry, Isfahan University of Technology, Isfahan 84156-83111, Islamic Republic of Iran

hydrophobicity, which are fabricated by direct carbonization of organic-organic nanocomposites [11]. OMCs are typically used as adsorbent in water treatment and gas storage purposes [10]. For instance, Koyuncu and Okur prepared a series of OMCs through the hard-templating method in a mesoporous silica template (KIT-6), and examined their efficiency in AV90 dye removal. The results revealed the maximum dye removal at pH 2 while the structure of OMCs maintained intact upon the adsorption processes [12].

FDU-15 is among the common OMCs used as a filler in polymer nanocomposites (NCs). With its sizeable pore volumes (0.65–0.85 cm³/g), high BET surface area (650–1500 m²/g), 2-D hexagonal structure, and hydrophobicity, FDU-15 serves beneficial in remediation of pollutants from water [10, 13]. Wu et al. have doped alkaline earth metals (including Mn, Sr, Ba and Ca) with FDU-15 and studied their capacity in nitrogen and oxygen removal. The results revealed that Mg had a significant adsorption capacity. The adsorption proceeded in either the conversion of nitrogen monoxide and oxygen to nitrogen dioxide and then to nitrite or direct oxidation of nitrogen monoxide to nitrite or nitrate [14].

However, there would be trouble in using FDU-15 as the reinforcing agent in the polymer matrix. The nature of FDU-15 is an obstacle to produce a homogenous composite since it is hydrophobic and cannot form bonds with the polar functional groups of the polymer and causes the agglomeration of the filler in the polymer matrix [15, 16]. Therefore, they must be modified with some coupling agents such as 3-aminopropyltriethoxysilane (KH-550) to decrease the agglomeration of mesoporous carbon into the polymer matrix. Mohammadnezhad et al. designed a series of NC films based on the PMMA and FDU-15 using 3-mercaptopropyl-trimethoxysilane as a modifying agent and studied their thermal stability and mechanical behaviors. The result showed that by increasing the amount of FDU-15, the thermal stability and their mechanical behavior rise as well [11].

KH-550 has been extensively used to make a bridge between inorganic fillers and the organic polymer matrix. On the one hand, the oxygen atom on its structure makes a covalent bond with the filler and on the other hand, the primary amine moiety reacts with the organic functional groups in the polymer matrix [17].

Ultrasonic irradiation as an efficient and green method has widely been exploited to achieve the maximum dispersion of fillers into the NCs. This helps the maximum interaction between polymer chains and nanoparticles become possible. In a study conducted by Mallakpour and his co-worker, a series of NCs based on chitosan-tragacanth blend reinforced with ZnO@Ag nanoparticles were prepared through ultrasonic irradiation. The result revealed that all the NCs were quite compatible with hydroxyapatite while they showed an extreme

antibacterial activity against both gram-negative and gram-positive bacteria [18].

In continuation to our previous report where the NCs were prepared from PMMA and m-FDU-15 [11], in this project, NCs were fabricated by in-situ polymerization of MMA in the presence of different (0.5, 1, 2, and 3) wt% of the modified FDU-15 (m-FDU). Fourier transform infrared spectroscopy (FT-IR) was used to detect functional groups, low angle X-ray diffraction (LXRD) was utilized to study the structure of mesopores, field emission scanning electron microscopy (FE-SEM) was employed for morphological investigation, and transmission electron microscopy (TEM) was used to observe the shape and dispersion of m-FDUs within the polymer matrix. Moreover, the influences of these mesoporous structures on the thermal stabilities of the PMMA based NCs were examined by thermogravimetric analysis (TGA).

Experimental

Materials

All the materials including P123 (triblock poly(ethylene oxide)-poly(propylene oxide)-poly(ethylene oxide), Mw = 5.8 × 10³), 3-aminopropyltriethoxysilane (KH-550), benzoyl peroxide (BP), methyl methacrylate (MMA, Mw = 100.117 g.mol⁻¹), n-decane, formaldehyde and toluene were acquired from the Merck and Aldrich Companies (Germany) and used as received.

Instruments

LXRD instrument (Bruker Nanostar U) with a wavelength of $\lambda = 0.1542$ nm, a voltage of 45 kV, and a flow of 100 mA was utilized to record the XRD patterns. The range of the collection was between 2 θ of 0.02° and 3.5° at a scanning rate of 0.05°/min. The thermal stability of samples in nitrogen atmosphere from the ambient temperature to 800 °C was investigated by the TGA instrument (model = NETZSCH STA 449F1, Germany). The surface morphology of the NCs was observed by FE-SEM (HITACHI, S-4160). TEM images were taken using a Philips CM120 (Eindhoven, Netherland).

Synthesis of mesoporous carbon FDU-15

Triblock copolymer (P123) and phenol/formaldehyde were used as a template and carbon precursors, respectively to synthesize the mesoporous carbon FDU-15 [19]. Briefly, at first, the exact amount of phenol (21 mmol)

and formaldehyde solution (7 mL, 40 wt%) were dissolved in 5 mL of 0.1 M NaOH. After that, 11 mmol of n-decane was poured into the solution of 3.2 g P123 in 50 mL of water. The mixture was continuously stirred for 5 h at 40 °C. After the addition of the phenol/formaldehyde solution, a white mixture was obtained. The color of the mixture changed to dark red as it was stirred for about 3 h at 65 °C and it even became darker after the process continued overnight at the same temperature. The rotation process was continued for the next three days and then the solution was stirred for an additional 24 h at 70 °C. The resulting sediments were collected and calcined in a tube furnace at 800 °C in an ambient pressure and N₂ atmosphere.

Preparation of m-FDU using KH-550 as a modifier

0.085 g of the dried FDU-15 (120 °C for 5 h) was mixed with KH-550 (0.04 mL) in ethanol (10 mL) and the mixture was stirred for 10 min. Then, the resultant suspension was sonicated for 1 h with the power of 70 W. Subsequently, the sonicated suspension was refluxed for 3 h and then was filtered and washed thoroughly with ethanol to remove unreacted KH-550. Finally, it was dried at 30 °C for 24 h.

In-situ preparation of PMMA/m-FDU-15 NCs

The following procedure was used to synthesize the PMMA-m-FDU NCs (0.5, 1, 2 and 3 wt%): predefined amounts of m-FDU were added to MA solutions in anhydrous toluene (9 mL) and were stirred and sonicated for 1 h using an immersed ultrasonic probe. After that, 0.03 g of benzoyl peroxide were added to the mixtures and refluxed for 6 h. Finally, the solutions were poured into a clean and smooth aluminum foil and let it dried overnight at 30 °C.

Results and discussion

Importance of substances, chemical agents, and methods

Using PMMA as a pure polymer would not be practical in most applications because of its vulnerability and its low thermal stability. One of the simplest solutions to improve these defects is the incorporation of fillers into the polymer matrix [20, 21]. Considering that every filler has its own properties, the polymer-based NCs can obtain those properties as well. For example, if a filler possesses thermal resistance or bioactivity, the resulting NC would have these abilities too [22]. FDU-15 depicts a significant surface/volume ratio and also is resistant to heat and temperature, therefore, incorporating this filler into the polymer matrix can result in an NC with improved thermal stability and the ability to adsorb pollutants such as heavy metals and dyes in the aqueous solution [1]. Moreover, it has been suggested that for maximizing the interaction between fillers and the functional group of the polymer matrix, some modifiers with at least two functional groups might become handy [23]. Also, ultrasonic irradiation can produce very tiny bubbles in the size of a micrometer with tremendous temperature which facilitates the process of modification of FDU-15 and KH-550 and improves the interaction between the m-FDU and the ester functional group of the polymer which results in a homogenous NC with the least agglomeration [24]. Figure 1 depicts a schematic representation of the possible interactions between FDU-15, KH-550, and PMMA matrix.

FT-IR spectroscopy

The FT-IR spectra of both FDU-15 and m-FDU are shown in Fig. 2. The strong absorption bands around 1600 (C–C stretching) and 1450 cm⁻¹ (C–H bending) which belong

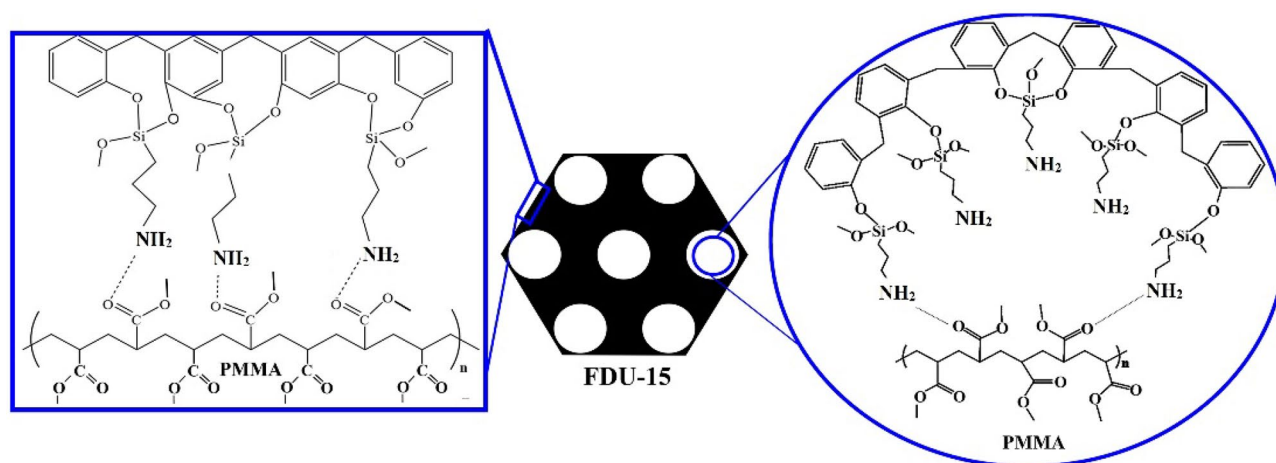


Fig. 1 The possible interactions between FDU-15 and PMMA matrix

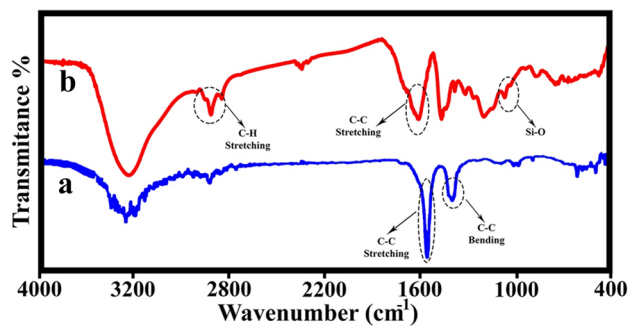


Fig. 2 The FT-IR spectra of a) FDU-15 and b) m-FDU

to the carbon materials confirm the synthesis of FDU-15 (Fig. 2a) [25]. The m-FDU also shows significant absorption peaks at 1060 cm^{-1} which is related to Si–O bonds [26]. The presence of both peaks at 1605 cm^{-1} and 1060 cm^{-1} , as well as 2852 and 2920 cm^{-1} bands of aliphatic C–H stretching, proves the successful modification of FDU-15 (Fig. 2b).

The FT-IR spectra of the PMMA and its related NCs are shown in Fig. 3. Two absorption bands in the area from 2900 cm^{-1} to 2950 cm^{-1} are related to asymmetric stretching vibrations of the aliphatic C–H bonds. Also, a very weak absorption peak at 2850 cm^{-1} is attributed to the vibrational absorption of the C–H bond in CH_3 . The carbonyl absorption stretching band of the ester functional group in the pure PMMA is observed at 1719 cm^{-1} . A strong absorption band at the area around 1240 cm^{-1} to 1270 cm^{-1} belongs to the different C–O stretching modes. Significant changes in the fingerprint area (400 cm^{-1} to 700 cm^{-1}) for the PMMA-m-FDU NCs are observable. These changes are the results of good interaction of m-FDU and the PMMA and successful preparation of the NCs. Also, the absorption band of the Si–O bond at 1080 cm^{-1} is another proof of successful fabrication of PMMA-m-FDU NCs [26].

LXRD patterns

The LXRD patterns of PMMA-m-FDU 0.5%, PMMA-m-FDU 1%, PMMA-m-FDU 2%, and PMMA-m-FDU 3 wt% are shown in Fig. 4. FDU-15 has a strong peak which is related to the (10) reflection and two weak peaks which are related to (20) and (21) reflections that is an indication of the $p6m$ symmetry [27, 28]. The diffraction patterns of modified FDUs also indicates a slight change in intensity and long range ordering upon modification [11, 15]. During the NCs preparation, FDU-15 porous framework is preserved and LXRD patterns of the NCs showed the main diffraction peak of the FDU-15 with lower intensities as expected. However, the incorporation process did not change the FDU-15 porous structure, the interaction of the

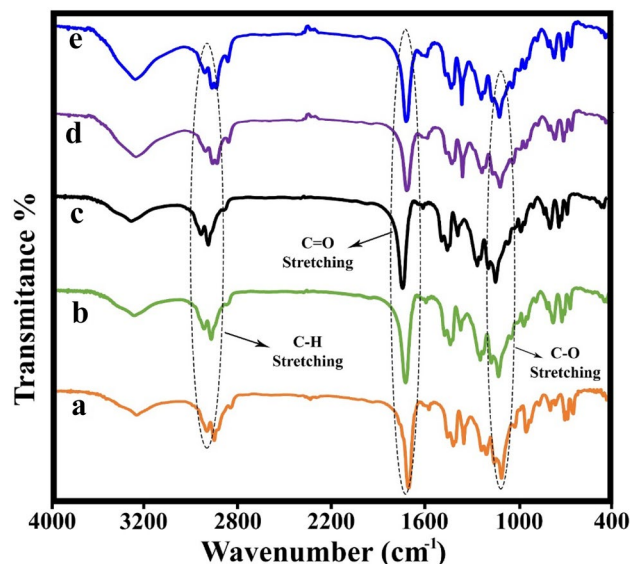


Fig. 3 The FT-IR spectra of a) PMMA, b) PMMA-m-FDU 0.5 wt%, c) PMMA-m-FDU 1 wt%, d) PMMA-m-FDU 2 wt%, and e) PMMA-m-FDU 3 wt%

filler and polymer matrix and pore filling has an effect on regularity and long range ordering of FDU-15 (Fig. 4.).

FE-SEM micrographs

Observation of the surface morphology of PMMA-m-FDU NCs was done by FE-SEM micrographs (Fig. 5). All the NCs show a unique dispersion of m-FDU on their surface. Moreover, the more the amount of the m-FDU increases,

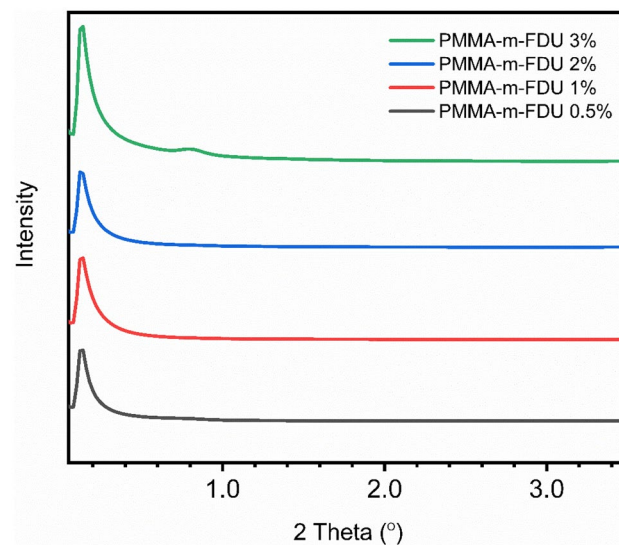
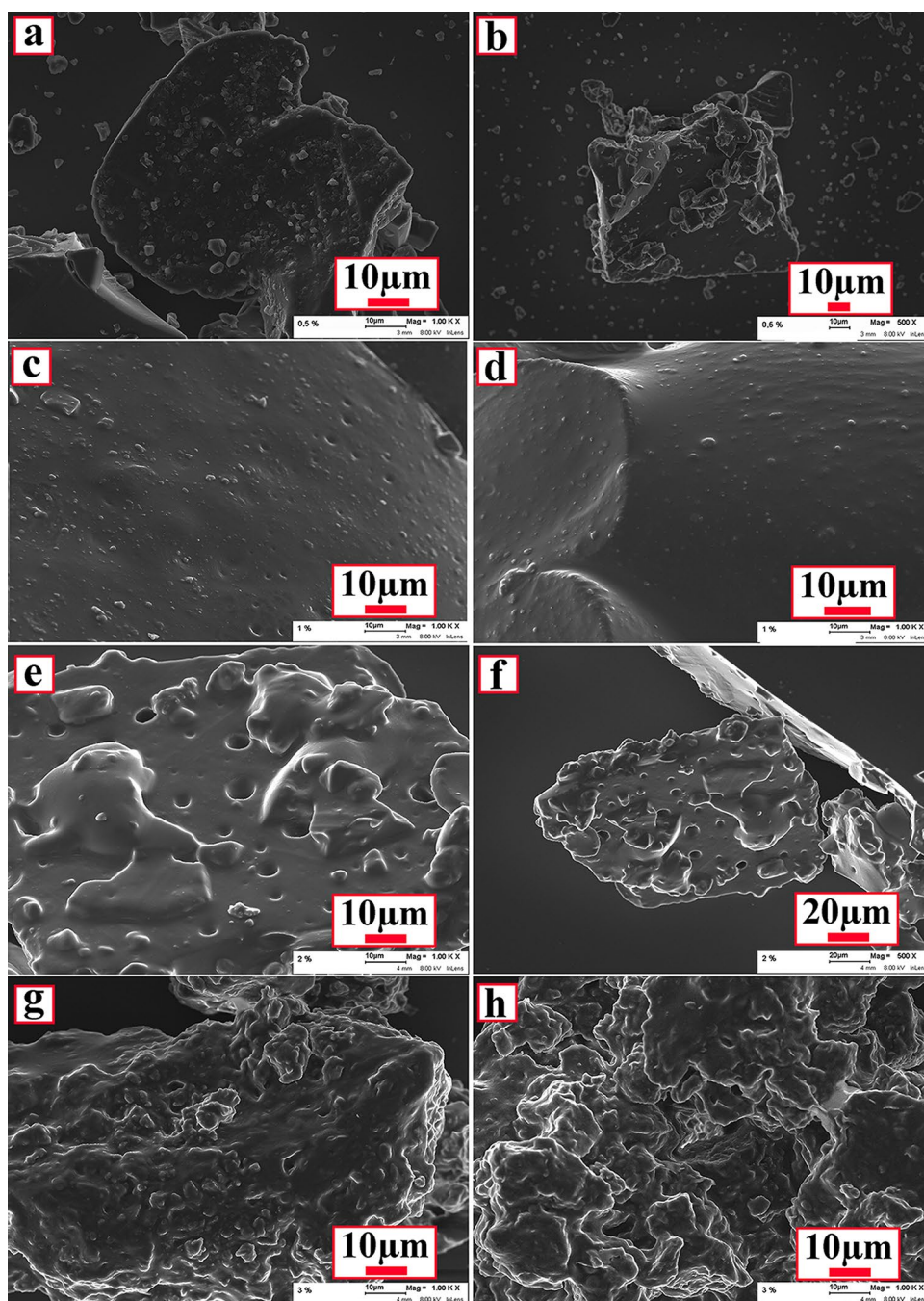


Fig. 4 The LXRD pattern of the PMMA-m-FDU 3%, PMMA-m-FDU 2%, PMMA-m-FDU 1%, and PMMA-m-FDU 0.5%

Fig. 5 FE-SEM Micrographs of **a, b**) PMMA-m-FDU 0.5 wt%, **c, d**) PMMA-m-FDU 1 wt%, **e, f**) PMMA-m-FDU 2 wt%, and **g, h**) PMMA-m-FDU 3 wt%



the surface of the NCs becomes rougher. The incorporation of m-FDU in the amounts of 1 wt% and 2 wt% has completely changed the morphology. The PMMA-m-FDU 1 wt% and PMMA-m-FDU 2 wt% show some pores on their surfaces, therefore it can be deduced that the surface area of these NCs has been increased as the amount of the m-FDUs rises (Fig. 5c-f). However, the surface morphology of the PMMA-m-FDU 3 wt% shows agglomeration of m-FDU on its surface (Fig. 5g, h). Therefore, the PMMA-m-FDU 2 wt% with the highest porosity was chosen as an optimum for further investigation.

TEM images of the PMMA-m-FDU 2 wt%

The TEM images of the PMMA-m-FDU 2 wt% are shown in Fig. 6. Ethanol was chosen for achieving the maximum dispersion of the NCs. Figure 6 shows the dispersed m-FDUs into the PMMA matrix with an average size of 22 nm which has been obtained by its related histogram (SPSS. Statics 17.0). Well dispersion of the m-FDUs into the polymer matrix might be the consequence of the better interactions between the mesoporous material and the PMMA matrix which could be the results of the in-situ polymerization of

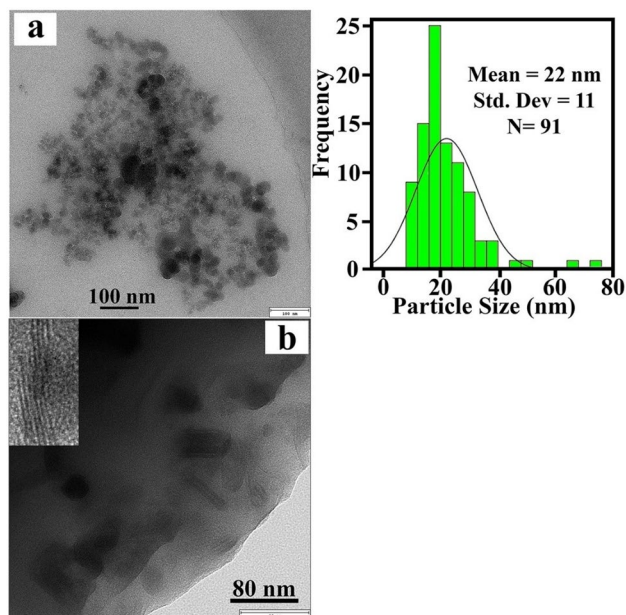


Fig. 6 The TEM images of the **a**) PMMA-m-FDU 2 wt% (100 nm) and **b**) PMMA-m-FDU 2 wt% (80 nm) inset: enlarged image viewed along [1 1 0] direction of the FDU-15

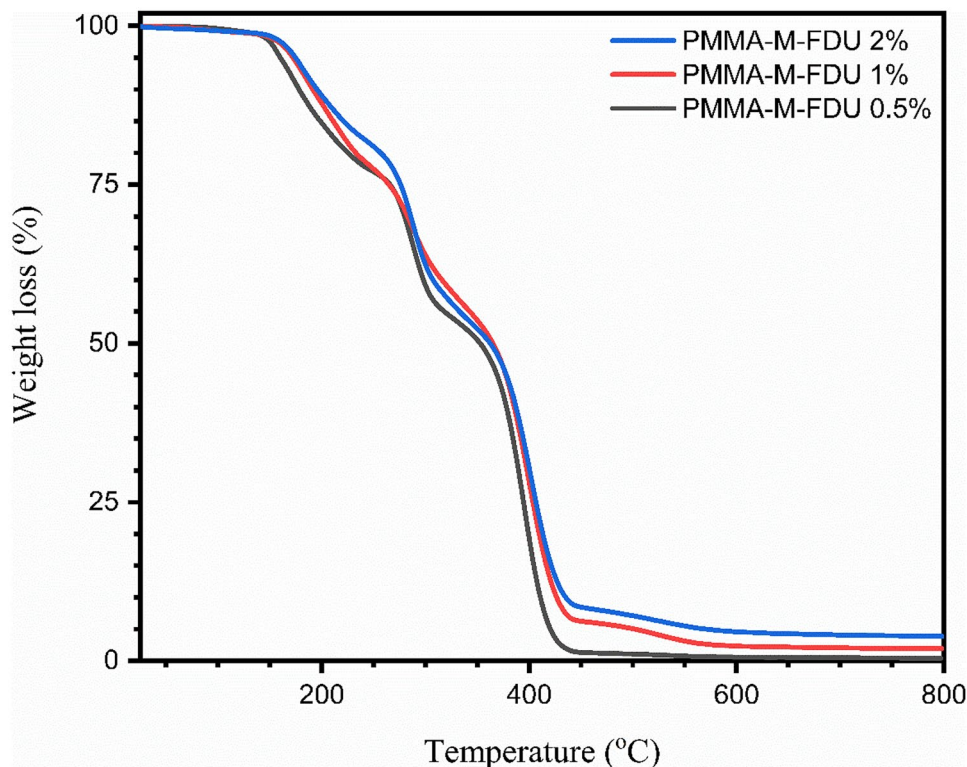
the MMA. The m-FDUs may act as nucleation points and therefore, they are dispersed into the matrix uniformly. In addition, it can be seen that there are some well ordered,

separated arrays with long fringes perpendicular to the pore axis that confirm the presence of the ordered FDU-15 with the $p6m$ symmetry (Fig. 6b inset).

TGA analysis

A study has proved that the pure FDU-15 has a negligible weight loss of around 5% even at the higher temperature, nearly 900 °C [28], while the m-FDU shows a significant weight loss (14.4 wt%) [13]. Figure 7 shows the TGA thermographs of PMMA NCs in the nitrogen atmosphere from the ambient temperature to 800 °C. Although they illustrate a relatively similar trend, a deeper look reveals some exact changes. Generally speaking, as the amount of the m-FDU increases in the matrix, the temperature of the decomposition steps rises as well and they shift to higher temperatures. For example, the T_d (the temperature when there is a 10 wt% loss of the sample) of the PMMA-m-FDU 0.5 wt%, PMMA-m-FDU 1 wt%, and PMMA-m-FDU 2 wt% were 179, 191 and 195 °C, respectively (Fig. 7). Therefore, the incorporation of m-FDU has resulted in higher thermal stability for the NCs, because of the indigenous thermal stability of the FDU-15 and the excellent interaction of these mesoporous structure and the PMMA matrix. The char yield (the total left over of the sample at 800 °C) of PMMA-m-FDU 0.5 wt%, PMMA-m-FDU 1 wt%, and PMMA-m-FDU 2 wt% were 0.5, 2, and, 4, %, respectively.

Fig. 7 The TGA thermographs of PMMA-m-FDU 0.5 wt%, PMMA-m-FDU 1 wt%, and PMMA-m-FDU 2 wt%



Conclusion

A series of NCs based on the PMMA as polymer matrix and the FDU-15 as nanoporous filler were fabricated via the in-situ polymerization method with the aid of ultrasonic irradiation. In this regards, the FDU-15 mesoporous structure was successfully synthesized by the use of P123 copolymer as the template and phenol/formaldehyde as a carbon precursor. Study of their functional groups, 2-D hexagonal structure of these unique mesopores, their morphology, and also their dispersion into the polymer matrix were investigated by the FT-IR, LXRD, FE-SEM, and TEM analysis, respectively. The TGA measurement revealed that the NCs with higher amount of m-FDU have higher thermal stability due to the better dispersion and better interactions between the mesoporous carbon and the matrix. Among all the samples, PMMA-m-FDU 2 wt% had a higher porosity and better thermal stability than those of the other NCs.

Acknowledgements The authors are thankful to the Research Affairs Division of Isfahan University of Technology (IUT) Isfahan, I. R. Iran.

Data availability All data generated or analysed during this study are included in this published article.

Declarations

Conflict of interest The authors declare that they have no known competing for financial interests or personal relationships that could have appeared to influence the work reported in this paper.

References

- Mohammadnezhad G, Moshiri P, Dinari M, Steiniger F (2019) In situ synthesis of nanocomposite materials based on modified-mesoporous silica MCM-41 and methyl methacrylate for copper (II) adsorption from aqueous solution. *J Iran Chem Soc* 16:1491. <https://doi.org/10.1007/s13738-019-01628-z>
- Hammani S, Barhoum A, Bechelany M (2017) Fabrication of PMMA/ZnO nanocomposite: effect of high nanoparticles loading on the optical and thermal properties. *J Mater Sci* 53:1911–1921. <https://doi.org/10.1007/s10853-017-1654-9>
- Aziz SB, Abdullah OG, Brza MA, Azawy AK, Tahir DA (2019) Effect of carbon nano-dots (CNDs) on structural and optical properties of PMMA polymer composite. *Results in Phys* 15:102776. <https://doi.org/10.1016/j.rinp.2019.102776>
- Bubmann T, Seidel A, Altstädt V (2019) Transparent PC/PMMA blends via reactive compatibilization in a twin-screw extruder. *Polymers* 11:2070. <https://doi.org/10.3390/polym11122070>
- Li YH, Shang XY, Li YJ (2020) Fabrication and characterization of TiMoCu/PMMA composite for biomedical application. *Mater Lett* 270:127744. <https://doi.org/10.1016/j.matlet.2020.127744>
- Singh G, Santhanakrishnan S (2021) Fabrication and characterization of composite PMMA/HA scaffold using freeze casting method. *Mater Technol* 1–8. <https://doi.org/10.1080/10667857.2021.1978640>
- Xu Y, Li D, Shen J, Guo S, Sue HJ (2019) Scratch damage behaviors of PVDF/PMMA multilayered materials: Experiments and finite element modeling. *Polymer* 182:121829. <https://doi.org/10.1016/j.polymer.2019.121829>
- Xu Y, Qin J, Shen J, Guo S, Lamnawar K (2021) Scratch behavior and mechanical properties of alternating multi-layered PMMA/PC materials. *Wear* 486:204069. <https://doi.org/10.1016/j.wear.2021.204069>
- Liu L, Meng WK, Li L, Xu GJ, Wang X, Chen LZ, Wang ML, Lin JM, Zhao RS (2019) Facile room-temperature synthesis of a spherical mesoporous covalent organic framework for ultrasensitive solid-phase microextraction of phenols prior to gas chromatography-tandem mass spectrometry. *Chem Eng J* 369:920. <https://doi.org/10.1016/j.cej.2019.03.148>
- Gang D, Uddin Ahmad Z, Lian Q, Yao L, Zappi ME (2021) A review of adsorptive remediation of environmental pollutants from aqueous phase by ordered mesoporous carbon. *Chem Eng J* 403:126286. <https://doi.org/10.1016/j.cej.2020.126286>
- Mohammadnezhad G, Dinari M, Soltani R, Bozorgmehr Z (2015) Thermal and mechanical properties of novel nanocomposites from modified ordered mesoporous carbon FDU-15 and poly(methyl methacrylate). *Appl Surf Sci* 346:182–188. <https://doi.org/10.1016/j.apsusc.2015.04.005>
- Eslek KD, Okur M (2021) Removal of AV 90 dye using ordered mesoporous carbon materials prepared via nanocasting of KIT-6: Adsorption isotherms, kinetics and thermodynamic analysis. *Sep Purif Technol* 257:117657. <https://doi.org/10.1016/j.seppur.2020.117657>
- Feng D, Li P, Feng Y, Yan Y, Zhang X (2021) Using mesoporous carbon to pack polyethylene glycol as a shape-stabilized phase change material with excellent energy storage capacity and thermal conductivity. *Microporous Mesoporous Mater* 310:110631. <https://doi.org/10.1016/j.micromeso.2020.110631>
- Wu R, Ye Q, Wu K, Dai H (2021) Low-temperature (NO + O₂) adsorption performance of alkaline earth metal-doped C-FDU-15. *J Environ Sci* 103:172–184. <https://doi.org/10.1016/j.jes.2020.10.014>
- Dinari M, Mohammadnezhad G, Nabiyan A (2015) Organo-modified mesoporous carbon FDU-15 as new nanofiller for the preparation of nanocomposite materials based on nylon-6. *Colloid Polym Sci* 293:1569–1575. <https://doi.org/10.1007/s00396-015-3556-1>
- Churipard SR, Kanakikodi MSP (2020) Metal Nanoparticles Supported on Mesoporous Polymers: Realizing the Synergetic Effect to Achieve Superior Catalytic Performance. *ACS Symp Ser* 1359:483–511. <https://doi.org/10.1021/bk-2020-1359.ch016>
- Sun L, Huang J, Liu H, Zhang Y, Ye X, Zhang H, Wu A, Wu Z (2018) Adsorption of boron by CA@KH-550@EPH@NMDG (CKEN) with biomass carbonaceous aerogels as substrate. *J Hazard Mater* 358:10–19. <https://doi.org/10.1016/j.jhazmat.2018.06.040>
- Mallakpour S, Okhovat M (2021) Hydroxyapatite mineralization of chitosan-tragacanth blend/ZnO/Ag nanocomposite films with enhanced antibacterial activity. *Int J Biol Macromol* 175:340. <https://doi.org/10.1016/j.ijbiomac.2021.01.210>
- Zhang F, Meng Y, Gu D, Yan Y, Chen Z, Tu B, Zhao D (2006) An aqueous cooperative assembly route to synthesize ordered mesoporous carbons with controlled structures and morphology. *Chem Mater* 18:5279–5288. <https://doi.org/10.1021/cm061400+>
- Zhu J, Abeykoon C, Karim N (2021) Investigation into the effects of fillers in polymer processing. *Int J Lightweight Mater Manuf* 4:370–382. <https://doi.org/10.1016/j.ijlmm.2021.04.003>
- Bacali C, Badea M, Moldovan M, Sarosi C, Nastase V, Baldea I, Chiorean RS, Constantiniuc M (2019) The influence of graphene in improvement of physico-mechanical properties in PMMA denture base resins. *Mater* 12:2335. <https://doi.org/10.3390/ma12142335>
- Mohammadnezhad G, Keikavousi Behbahan A (2020) Polymer matrix nanocomposites for heavy metal adsorption: a

- review. *J Iran Chem Soc* 17:1259–1281. <https://doi.org/10.1007/s13738-020-01864-8>
23. Fu S, Sun Z, Huang P, Li Y, Hu N (2019) Some basic aspects of polymer nanocomposites: A critical review. *Nano Mater Sci* 1:2–30. <https://doi.org/10.1016/j.nanoms.2019.02.006>
 24. Dong X, Liang X, Zhou Y, Bao K, Sameen DE, Ahmed S, Dai J, Qin W, Liu Y (2021) Preparation of polylactic acid/TiO₂/GO nanofibrous films and their preservation effect on green peppers. *Int J Biol Macromol* 177:135. <https://doi.org/10.1016/j.ijbiomac.2021.02.125>
 25. Trick KA, Saliba TE (1995) Mechanisms of the pyrolysis of phenolic resin in a carbon/phenolic composite. *Carbon* 33:1509–1515. [https://doi.org/10.1016/0008-6223\(95\)00092-R](https://doi.org/10.1016/0008-6223(95)00092-R)
 26. Kathi J, Rhee KY (2008) Surface modification of multi-walled carbon nanotubes using 3-aminopropyltriethoxysilane. *J Mater Sci* 43:33–37. <https://doi.org/10.1007/s10853-007-2209-2>
 27. Meng Y, Gu D, Zhang F, Shi Y, Yang H, Li Z, Yu C, Tu B, Zhao D (2005) Ordered mesoporous polymers and homologous carbon frameworks: amphiphilic surfactant templating and direct transformation. *Angew Chem Int Ed* 44:7053–7059. <https://doi.org/10.1002/anie.200501561>
 28. Wu Z, Webley PA, Zhao D (2010) Comprehensive study of pore evolution, mesostructural stability, and simultaneous surface functionalization of ordered mesoporous carbon (FDU-15) by wet oxidation as a promising adsorbent. *Langmuir* 26:10277–10286. <https://doi.org/10.1021/la100455w>

Publisher's Note Springer Nature remains neutral with regard to jurisdictional claims in published maps and institutional affiliations.